Effect of silicon addition on deformation mechanisms of near alpha titanium alloys

Thibaut Armanni, Frédéric Fossard, Jean-Sébastien Mérot, Thierry Douillard, Camille Liard, Zhao Huvelin, Benoît Appolaire

EFFECT OF SILICON ADDITION ON DEFORMATION MECHANISMS OF NEAR-ALPHA TITANIUM ALLOYS

Thibaut Armanni[1], Frédéric Fossard[2], Jean-Sébastien Mérot[2], Thierry Douillard[3], Camille Liard[1], Zhao Huvelin[1], Benoît Appolaire[4, 5]

[1] *Université Paris Saclay, ONERA, Matériaux et Structures, 92322, Châtillon, France*
[2] *Université Paris-Saclay, ONERA, CNRS, Laboratoire d'étude des microstructures, 92322, Châtillon, France*
[3] *INSA Lyon, Université de Lyon, MATEIS, UMR CNRS 5510, F69621 Villeurbanne, France*
[4] *Université de Lorraine, CNRS, Institut Jean Lamour, Nancy, France*
[5] *Labex DAMAS, Université de Lorraine, France*

In this paper we investigate the mechanism of strengthening in Si reinforced Ti6244 alloys. As the beneficial or detrimental effect of silicide precipitation is still debated, we bring some deeper understanding of the effect of Si in near-α titanium alloys. In order to provide some insights, extensive characterizations have been carried out at two scales: the effect of Si has been analyzed with multiple tensile tests at room temperature and at 650 °C; then, the population of silicides has been analyzed on as received or aged samples by FIB-SEM 3D reconstruction, to determine their morphology, size and distribution; and also by TEM, to identify the nature of the precipitates as well as their interaction with dislocations. We show that by playing with the silicon content we observe copious precipitation of silicides. And that they play an important role in the high temperature mechanical properties (creep) following an Orowan mechanism.

Keywords: Near-alpha, Silicides, Mechanical properties, TEM, FIB-SEM, CalPhaD

1. Introduction

Reducing pollutant emissions is a major strategic challenge for the aerospace industry. Materials have an important role to play in developing innovative solutions for 'greener' aviation. The current needs clearly identified are the following: to increase the temperature properties of materials and to reduce the overall weight of the aircraft. In the field of metallic materials, titanium alloys offer excellent specific mechanical strength and good corrosion resistance. These features make them particularly competitive with steels and nickel-based superalloys up to temperatures around 550 °C.

These Ti alloys are used in aircraft engines, particularly in compressor blades and discs, casings, and structural parts, such as engine pylons and landing gear. The expected increase in performance of future aircraft turbomachinery will inevitably lead to an increase in operating temperatures, particularly in the compressor parts, and will have an impact on the pylon. One of the main challenges for the aerospace industry is to improve the temperature resistance of titanium alloys.

The titanium alloys traditionally used at high temperatures are alloys of the so-called "*near-α*" category. Ti6242 is emblematic, as it contains a significant proportion of the hexagonal phase, which ensures a satisfactory resistance at high temperatures. However, these near-α alloys, such as Ti6242 or Ti834 used in the discs of turbomachinery compressors, are very sensitive to fatigue-creep stresses at room temperature, commonly known as the "*dwell effect*" [1].

The sensitivity of these alloys to the dwell effect is known to be related to the microstructure and microtexture of the α phase in the alloy [2]. It decreases significantly with increasing molybdenum content [3].

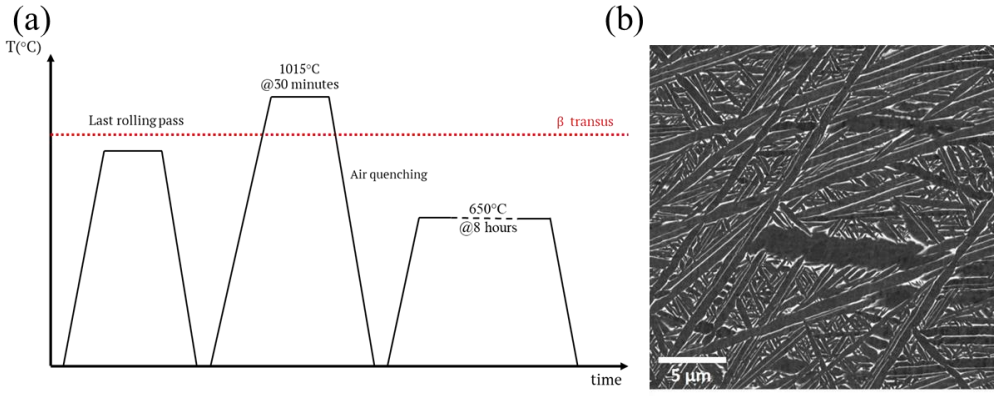

Figure 1 - As-received state, (a) thermal state and (b) microstructure.

According to Qiu et al [3], an increase in Mo content would promote the formation of thin α-phase laths of different crystallographic variants, leading to the formation of an entangled microstructure that is much less sensitive to the dwell effect. Unfortunately, since Mo is a β-stabilizing element, increasing its content leads to an increase in the β-phase fraction and a decrease in high temperature performance, in terms of mechanical strength or creep resistance. In order to counteract this decrease in mechanical properties at high temperatures, the addition of silicon has been proposed. Indeed, it is well known [4]-[9] that silicon content significantly improves the creep resistance of near-α alloys. However, the strengthening mechanism of silicon is still under discussion.

The purpose of this study is to provide a deeper understanding of the effect of Si in near-α titanium alloys using Scanning Electron Microscope (SEM), Focused Ion Beam (FIB)-SEM, Transmission Electron Microscope (TEM), tensile tests and CalPhaD calculations.

2. Materials and experiments

Arc melted 350 g buttons of a near-α alloy, Ti-6Al-2Sn-4Zr-4Mo-(0 to 0.23) Si wt %., were produced, hot rolled and then solution treated in the β-phase field with quenching in air at room temperature followed by annealing at 650 °C for 8 h (as-received condition). A lamellar microstructure was obtained with α phase lamellae (hcp) distributed in a beta matrix (cc). The as-received heat treatment (suffix _AR) and the microstructure at this stage are shown in Figure 1 (a-b). In addition, some samples were aged at 650 °C for 120 h (suffix _V650). The alloys were provided by TIMET. Sample designation and chemical composition are given in Table 1.

The samples observed were taken from the center of the rod. They were mechanically polished with silicon carbide paper from 300 to 1200-grit, a 9 and 3 µm diamond suspension, and finally with a 0.02 µm colloidal silica suspension in a vibratory polisher (Buehler VibroMet 2).

Table 1 - Alloy designations and chemical compositions (wt.%) obtained by Inductively Coupled Plasma (ICP) analysis.

	Al	Sn	Zr	Mo	Si	O
Ti6244 (0 wt.% Si)	5.8	2.1	4.1	3.8	0	0.12
Ti6244S (0.115 wt.% Si)	5.6	2.0	4.0	3.7	0.12	0.12
Ti6244S2 (0.23 wt.% Si)	5.7	2.1	4.1	3.7	0.23	0.12

Microstructural investigations of as-received and heat-treated specimens were carried out using a TESCAN MIRA3 FEG-SEM operated at 5 kV in BSE mode. 3D reconstruction was performed using a ZEISS NVISION FIB/SEM. We targeted cubic voxels with a side length of 5 nm. To obtain information from the very surface, BSE/SEM images were taken at 1.5 kV. Image analysis was performed using Image J software with the following packages: “Ellipse split” and “MorphoLibJ”.

To isolate small precipitates, site-specific thin lamellae were lifted out using a ThermoFisher HELIOS 660 SEM/FIB system. STEM characterization of fine precipitates was performed using a TITAN G2 probe corrected S/TEM operating at 300 kV and equipped with high-angle annular dark field (HAADF) and Super X Energy Dispersive Spectroscopy (EDS) detectors.

Tensile specimens were taken from the center of the rod and were 4 mm in diameter and 30 mm in length. These tests were performed in air at 20 and 650 °C using an Instron 5582 testing machine at a strain rate of 2.10^{-4} s^{-1}.

The CalPhaD calculations were performed using the TCTI1 database.

3. Results and discussion

Figure 2 shows the effect of silicon on the stress-strain curves of three different alloys at 20 and 650 °C for both thermal states.

On the as-received specimens, at 20 and 650 °C, the 0.2% offset yield strength (0.2% OYS) and the ultimate tensile strength (UTS) of the Ti6244S2 alloy are increased by approximately 10% compared to the alloy without silicon. Conversely, the total elongation at fracture at 20 °C is reduced by approximately 40%. On the other hand, the alloy with 0.115 wt. % Si does not differ significantly from the alloy without silicon.

On the aged samples, the effect of Si is already observed on the 0.115 wt. % Si for both temperatures. Indeed, 0.2% OYS and UTS are increased by approximately 3% compared to the alloy without Si. The effect of Si is more visible on the total elongation at fracture, which is reduced by about 30% at 20 °C. The alloy with the highest Si content also shows a modification of its mechanical properties. Indeed, at 20 and 650 °C, these 0.2% OYS and UTS are increased by about 5% compared to the alloy without Si. The effect of the addition of Si is more visible on the total elongation at fracture, which is reduced by about 35% at 20 °C. It is also interesting to note a slight decrease in UTS and 0.2% OYS on the Si-rich alloy before and after ageing.

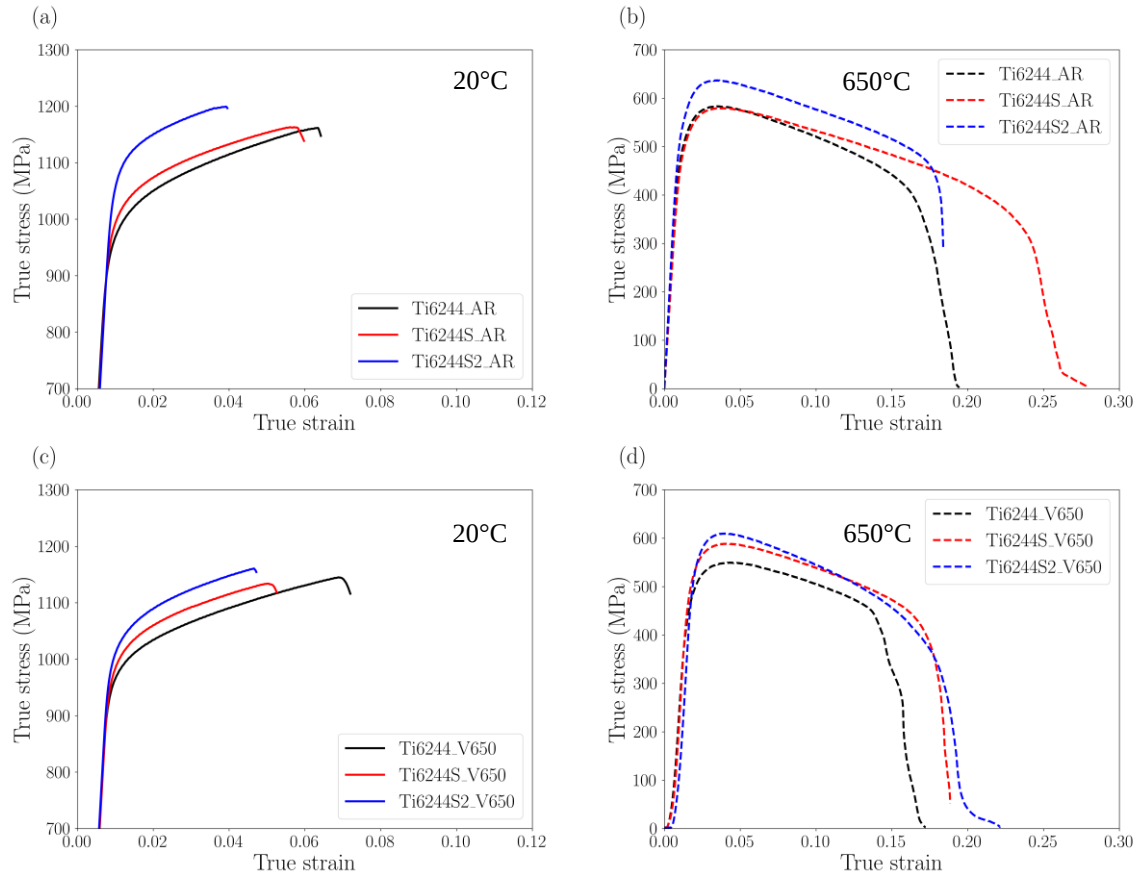

Figure 2 – Stress – strain curves of the as-received samples at (a) 20 °C, (b) 650 °C and of the aged samples at (c) 20 °C, (d) 650 °C.

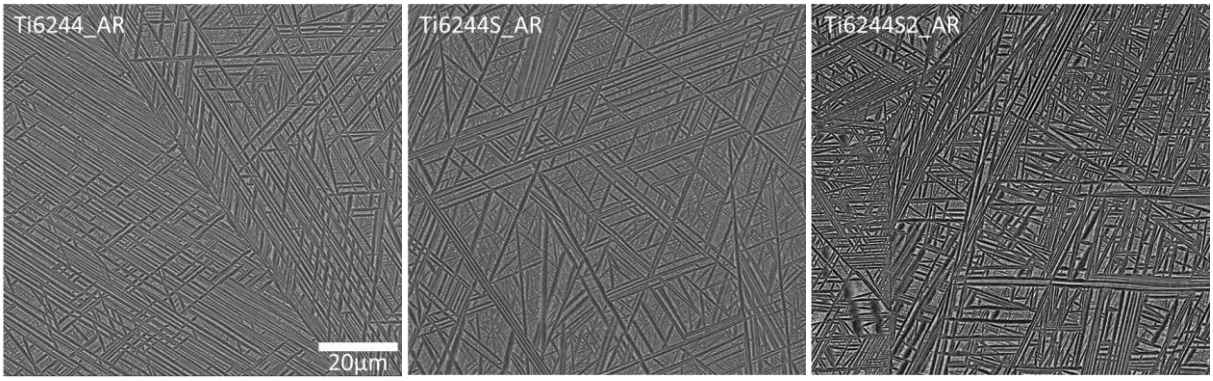

Figure 3 – Microstructure in the as-received state of Ti6244 with different silicon contents (0 to 0.23 wt. %).

Despite these differences in mechanical properties, Figure 3 shows similar lamellar microstructures on alloys containing silicon variations. These alloys have almost the same α fraction and lamellar width (Figure 3 and Table 2): the addition of Si does not appear to play a significant role on the formation of α. During ageing, the volume fraction of a increases by approximately 10% to get closer to the equilibrium values predicted by CalPhaD calculations with TCTI1 database (Table 2).

With optimal BSE-SEM parameters, it is possible to observe some bright precipitates at the α/β interface. However, these precipitates can only be observed in the alloys with modified tensile properties (Ti6244SV650, Ti6244S2_AR and Ti6244S2_V650).

It is well known that above critical levels, depending on the alloy, and during prolonged ageing, silicon leads to the precipitation of different silicides M_3Si, M_5Si_3 or M_6Si_3 [9]-[11]. Their effect on the mechanical properties

is not clearly established in the literature [4]-[9]. However, the results obtained in this study show that they would increase 0.2% OYS and UTS at room and high temperature and correlatively reduce ductility.

To confirm this relationship between silicides and properties, we have characterized the microstructures by various microscopic means. We carried out 3D reconstructions of the microstructure by SEM/FIB (Figure 4a) on the alloys in the aged state. The mean size of the silicides was extracted from a population of nearly 4 000 precipitates obtained on both alloys (Figure 4b). The amount of silicon in solid solution is assumed to be identical in both samples. It is therefore possible to associate the nominal composition with a significant difference in the proportion of silicides (Figure 5a-b). The Si rich alloy has 5 times more silicides, which is an important finding to explain the strengthening by Si. The same trends are predicted by CalPhaD calculations (Figure 5c-d).

Table 2 – Volume fraction of α phase (%) in the Ti6244x alloys using image analysis and CalPhaD calculations.

	As-received (AR)	**Aged** (V650)	**TCTI1**
Ti6244	70.7 (± 2.4)	81.9 (± 0.4)	88.2
Ti6244S	73.6 (± 0.9)	79.9 (± 0.4)	87.9
Ti6244S2	69.8 (± 2.7)	80.4 (± 2.4)	87.2

Using TEM observations, we have highlighted the interaction between silicides and dislocations (Figure 6b-c). We have also determined the nature of the silicide/α interfaces (Figure 6d), either coherent or semi-coherent, depending on the size of the precipitates. Figure 6(c) illustrates the interaction of dislocations and silicides, in a sample in the as-received state. We observe the presence of dislocation loops around the precipitates, presumably semi-coherent, which would have formed during crossing by an Orowan mechanism. Furthermore, from TEM observations of the most Si-rich alloy in the as-received and aged states, we have highlighted the significant growth of the silicides during the ageing process, going from a Feret diameter of 44 nm to 77 nm. It is well known [12] that the bypassing of precipitates by dislocations is effective beyond a critical size, independent of the volume fraction of the precipitates, but strongly dependent on the nature of the precipitates and their interfaces. In the bypass regime, the hardening decreases in a manner inversely proportional to the size of the precipitates, at a constant volume fraction. Therefore, it seems plausible to attribute the evolution of the size of the silicides to the slight deterioration of the mechanical strength of the alloys observed at the end of the ageing process.

Finally, the TEM-EDS analysis (Figure 6a) shows small zirconium enriched precipitates of the $M(Ti, Zr)_xSi_y$ type in the alloy with 0.23 wt. % in the aged condition.

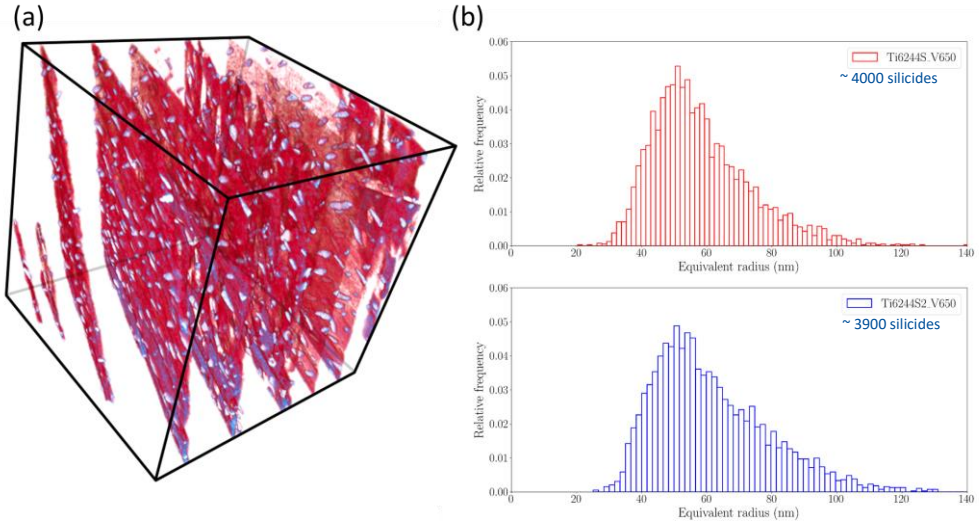

Figure 4 – (a) 3D reconstruction of the microstructure by SEM/FIB with beta phase thresholding (red) and silicide thresholding (blue) and (b) precipitate size distributions determined from these characterizations.

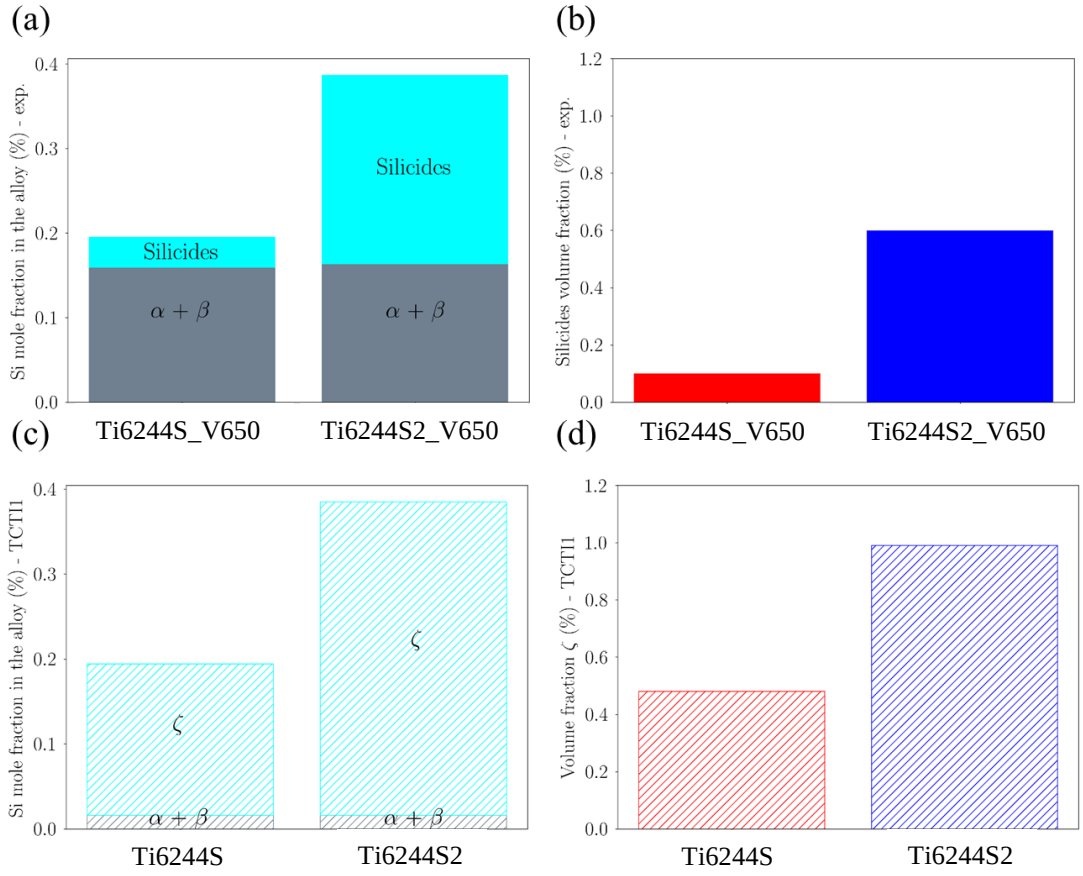

Figure 5 (a-b) Quantifications from 3D SEM/FIB reconstructions: (b) Si content of phases; (b) volume fraction of silicides. (c-d) Predictions from Thermo-Calc and TCTI1: (c) Si content of phases; (d) volume fraction of silicides.

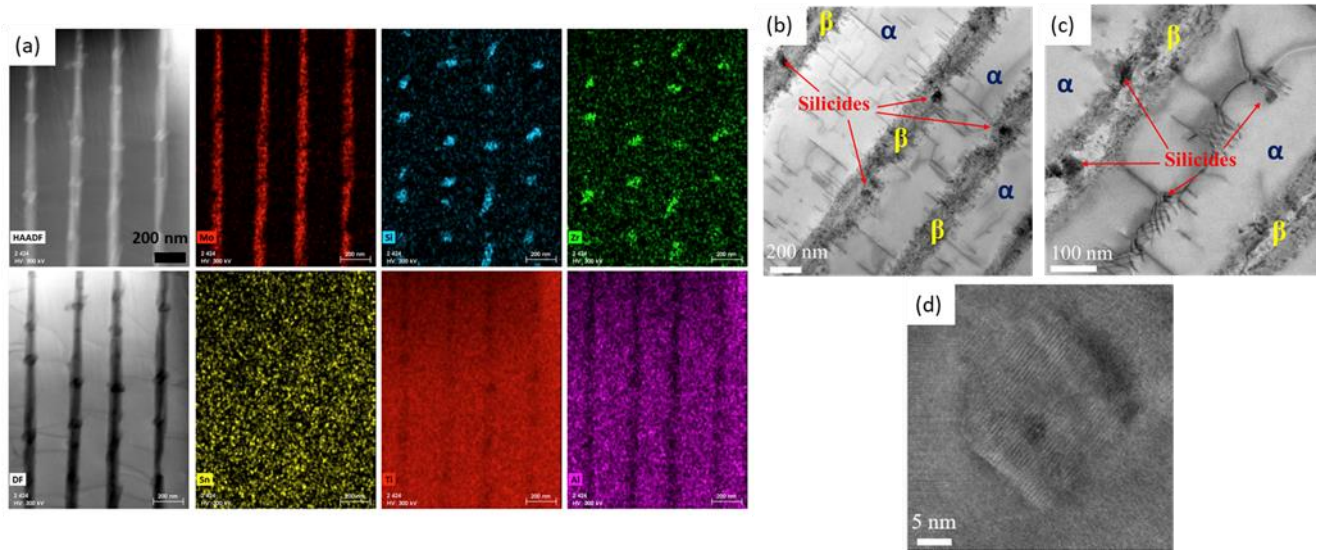

Figure 6 –TEM analysis, (a) EDS elemental, STEM HAADF and DF reference images; (b, c) annular bright field STEM images; (d) far field HR-STEM image of a precipitate in the α phase of 0.23 wt. % Si alloy in the as-received condition.

4. Conclusions

The effect of silicon addition on the deformation mechanisms of near-α titanium alloys Ti-6Al-2Sn-4Zr-4Mo-(0 to 0.23) Si %wt. has been investigated and led to the following conclusions.

1. The addition of Silicon increases the 0.2% OYS and UTS of these alloys at 20 and 650°C, and correlatively reduces the ductility at room temperature.
2. The main microstructural difference observed by SEM and TEM analysis is the presence of silicides in the alloys.
3. FIB-SEM analysis and CalPhaD calculations confirm that the only difference between the alloys is the volume fraction of the precipitates and not the amount of silicon in solid solution. The increase in mechanical properties is due to a precipitation strengthening mechanism.
4. TEM analysis reveals interactions between dislocations and silicides. The observation of loops around them and the incoherence of some precipitates (depending on their size) suggest an Orowan mechanism.

Acknowledgements

This work is part of the ALTITUDE project supported by the French National Research Agency (ANR-18-CE08-0024-01). The authors are also grateful for the financial support of the French METSA network (FR3507) for SEM/FIB experiments at the CLYM facilities. Finally, we would like to warmly thank Dr Shigehisa Naka for sharing his knowledge during many enlightening discussions.

References

[1] Evans, W.J., Gostelow, C.R., Metallurgical Transactions A 10 (1979) pp. 1837-1846.
[2] Bache M., International Journal of Fatigue 25 (2003) pp. 1079–1087.
[3] Qiu, J., Ma, Y., Lei, J., Liu, Y., Huang, A., Rugg, D., Yang, R., Metallurgical and Materials Transactions A 45 (2014) pp. 6075–6087.
[4] Paton, N.E., Mahoney, M.W., Metallurgical Transactions A 7 (1976) pp. 1685–1694.
[5] Assadi, A.T.K., Flower, H.M., West, D.R.F., Metals Technology, 6 (1979) pp. 16–23.
[6] Singh, V. and Ramachandra, C., Key Engineering Materials 8 (1985) pp. 185–202.
[7] Ramachandra, C., Singh, V. and Rao, P.R., Defence Science Journal 36 (1986) pp. 207–220.
[8] Neal, D.F., Fox, S.P., Titanium 92 (1992) pp. 287–294.
[9] Banerjee, D., Williams, J.C., Acta Materialia 61 (2013) pp. 844–879.
[10] Salpadoru, N.H., Flower, H.M., Metallurgical and Materials Transactions A 26 (1995) pp. 243–257.
[11] Azevedo, C.R.F., Flower, H.M., Calphad 26 (2002) pp. 353–373.
[12] Friedel, J., Dislocations, Pergamon (1964).